Development of a Single-Column Model in RegCM4 and Its Preliminary Application for Evaluating PBL Schemes in Simulating the Dry Convection Boundary Layer

Article *in* Journal of Tropical Meteorology · September 2021

DOI: 10.46267/j.1006-8775.2021.023

2 authors:

Zhenyu Han
China Meteorological Administration
91 PUBLICATIONS **1,635** CITATIONS
SEE PROFILE

Yuxing Wang
State Oceanic Administration
10 PUBLICATIONS **142** CITATIONS
SEE PROFILE

Article ID: 1006-8775(2021) 03-0259-13

Development of a Single−Column Model in RegCM4 and Its Preliminary Application for Evaluating PBL Schemes in Simulating the Dry Convection Boundary Layer

HAN Zhen-yu (韩振宇)[1], WANG Yu-xing (王宇星)[2]
(1. National Climate Center, China Meteorological Administration, Beijing 100081 China;
2. National Marine Hazard Mitigation Service, Ministry of Natural Resources, Beijing 100194 China)

Abstract: A single-column model (SCM) is developed in the regional climate model RegCM4. The evolution of a dry convection boundary layer (DCBL) is used to evaluate this SCM. Moreover, four planetary boundary layer (PBL) schemes, namely the Holtslag-Boville scheme (HB), Yonsei University scheme (YSU), and two University of Washington schemes (UW01, Grenier-Bretherton-McCaa scheme and UW09, Bretherton-Park scheme), are compared by using the SCM approach. A large-eddy simulation (LES) of the DCBL is performed as a benchmark to examine how well a PBL parameterization scheme reproduces the LES results, and several diagnostic outputs are compared to evaluate the schemes. The results show that the SCM is properly constructed. In general, with the DCBL case, the YSU scheme performs best for reproducing the LES results, which include well-mixed features and vertical sensible heat fluxes; the simulated wind speed, turbulent kinetic energy, entrainment flux, and height of the entrainment zone are all underestimated in the UW09; the UW01 has all those biases of the UW09 but larger, and the simulated potential temperature is not well mixed; the HB is the least skillful scheme, by which the PBL height, entrainment flux, height of the entrainment zone, and the vertical gradients within the mixed layer are all overestimated, and a inversion layer near the top of the surface layer is wrongly simulated. Although more cases and further testing are required, these simulations show encouraging results towards the use of this SCM framework for evaluating the simulated physical processes by the RegCM4.

Key words: single-column model; RegCM4; dry convection boundary layer; boundary layer schemes
CLC number: P46 **Document code:** A
https://doi.org/10.46267/j.1006-8775.2021.023

1 INTRODUCTION

Although climate numerical models have had a great development in recent years, many physical processes such as turbulent and diffusion processes in the planetary boundary layer (PBL) still cannot be fully resolved partly due to coarse resolution. Therefore, physical parameterization is indispensable and critical to these models, and parameterization testing is a vital task in model development. The easiest and most widely used approach is by application of climate simulations, the results of which can be directly compared with multiple observations or reanalysis datasets. However, one disadvantage is that it can be very difficult to attribute simulation deficiencies to particular aspects of a model's formulation because various feedbacks, such as the interplay between dynamics and physics, are mingled together during model integration [1]. The single-column model (SCM) is an economical framework for developing and diagnosing the physical processes in climate models, and with this tool, a parameterization can be tested by evaluating its ability to reproduce the observed tendencies for a given large scale situation.

Several regional climate modeling (RCM) or limited area modeling (LAM) groups have constructed SCMs (Table 1). Of the various RCMs that have been applied over China or the East Asia region, the RegCM series is one of the most commonly used [2−7]. The ARCSyM, which is an Arctic version of RegCM2, has an SCM called ARCSCM [8]; however, this SCM has not been integrated into the RegCM4's released versions. There has been no reported SCM for the regional climate model RegCM4 until now. In this study, an SCM is developed with most of the parameterizations inherited from the RegCM4. For ease of construction and use, this SCM is designed exactly following the framework of the original RegCM4 with three dimensions (3D).

There is no absolute best PBL parameterization scheme because each scheme have both advantages and

Received 2021-05-11 **Revised** 2021-05-15 **Accepted** 2021-08-15
Funding: National Key R&D Program of China (2018YFA0606301; 2020YFA0608201; 2017YFA0605004); National Natural Science Foundation of China (41405101)
Biography: HAN Zhen-yu, Associate Professor, primarily undertaking research on regional climate modeling and climate change.
Corresponding author: WANG Yu-xing, e-mail: yuxing.wang@foxmail.com

Table 1. Information regarding some regional climate models (RCM) and limited area models (LAM) with the single-column model implementation.

RCM/ LAM	ARCSyM	GRAPES_Meso	GRIMs	HIRLAM/HARMONIE	MM5	WRF
Institution	University of Colorado, US	China Meteorological Administration, China	Yonsei University, South Korea	Several National Meteorological Services in Europe	Pennsylvania State University and NCAR, US	NCAR, US
Reference	Morrison et al. [8]	Yang and Shen [9]	Hong et al. [10]	Neggers et al. [11]	Deng et al. [12]	Hacker and Angevine [13]

disadvantages contributing to various assumptions and formulations [14–15]. Therefore, a deep understanding of the physical behavior of PBL schemes will help improve PBL parameterizations and interpret simulation deficiencies. Then, the constructed model in this study is used in sensitivity studies of SCM simulations for the PBL schemes.

To assess the performance of a PBL scheme, well-controlled cases are usually used to isolate the contribution of PBL processes, which are either ideal cases or simplified real cases. A previous evaluation of PBL schemes in the SCM framework of the Community Atmosphere Model (CAM) by Bretherton and Park [16] focused on three types of PBLs: (1) the dry convection boundary layer (DCBL), (2) stably stratified boundary layer, and (3) nocturnal stratocumulus-topped boundary layer, which have also been widely used as testbeds in past intercomparison studies. The first purpose of this study is to test if the SCM has been correctly constructed, and thus, the most fundamental case of the DCBL is chosen. Based on this case, the basic performances of the four different PBL schemes are also evalulated.

The large-eddy simulation (LES) models can robustly reproduce observed DCBLs without significant model dependence, and have been widely used as benchmarks [13–18]. We first simulated the evolution of a DCBL using a LES model. Then, the SCM with each PBL parameterization scheme is driven by the same prescribed surface heat fluxes and initial conditions as those of the LES run. The PBL characteristics simulated from the SCM runs are compared with each other and with those derived from the LES data.

In Section 2, the DCBL simulation sets of both the LES and SCM, construction of the SCM, and brief summary of the PBL schemes used in this study are described. The evaluations of the simulated PBL features from the SCM are presented in Section 3, and in Section 4, a summary is provided.

2 MODEL, EXPERIMENTAL DESIGN, AND METHOD

2.1 *LES benchmark simulation*

The University of California, Los Angeles, large-eddy simulation (UCLA-LES [19]) model is used to simulate a DCBL explicitly. The design of this DCBL case follows the study by Bretherton and Park [16]. The PBL flow is driven by the prescribed surface sensible heat flux of 300 W m^{-2}, and the surface temperature is derived based on the flux-gradient relation, with the roughness set to 0.1 m . The initial profiles are set with a potential temperature of $\theta = 288\ \mathrm{K} + (3\ \mathrm{K\ km^{-1}}) \times z$ and the wind component values are $u = 10\ \mathrm{m\ s^{-1}}$ and $v = 0\ \mathrm{m\ s^{-1}}$. The surface pressure is set to 1000 hPa within the whole simulation period. The Coriolis acceleration is turned off, and there is no moisture, large-scale vertical motion, or radiative heating.

The resolution set uses the typical configuration, including that the horizontal extent covers the domain of 10 × 10 km^2 with 50-m resolution; the vertical extent reaches a height of 5 km with 20-m resolution; a sponge layer occupies the upper ten levels. A 16-h-long simulation is conducted, with the first hour being excluded from the analysis as model spin-up. The instantaneous fields over time and over different heights are averaged to derive 5-min and hourly mean variables.

2.2 *SCM model construction*

Most parts of the SCM, including the dynamic core and physics packages are the same as those of the 3D RegCM4 (model version v4.4). To minimize changes in the original codes (e.g., staggered Arakawa B-grid), a 4 × 4 grid but not a single vertical column is set as the dynamic core of the SCM. On this 4 × 4 grid, all horizontal dynamical processes (horizontal diffusion and advection) and lateral boundary conditions are turned off, but the cyclic boundary conditions in both the x and y directions are added, and thus, the values of all variables are the same among those grid points. Then, any point from this 4 × 4 grid can be considered a "single column".

As with other SCMs (e. g., SCMs in WRF and CAM), horizontal temperature and moisture advective tendencies, as well as vertical velocity or vertical advection, can be prescribed as inputs to drive the SCM. However, all these modules are switched off in this study.

2.3 *SCM simulations*

To ensure that the discrepancies in the simulated

PBL flow are only due to differences in the PBL schemes, only the PBL and surface layer parameterization along with dry dynamical core are activated in the DCBL simulation run. The four PBL schemes used in this paper are the Holtslag-Boville scheme (HB) [20–21], Yonsei University scheme (YSU) [22–23], and two University of Washington schemes (UW01 and UW09). The UW01 is based on Grenier and Bretherton [24] and Bretherton et al. [25], while the UW09 is based on Bretherton and Park [16]. The HB has been part of the RegCM series models since the early version, the UW01 was added to the RegCM4 by O'Brien et al. [26], and the YSU and UW09 is added by the authors of this study, and the codes are modified from the WRF v3.5.1 and CESM v1.2.0 models, respectively.

The HB and YSU are the non-local, first-order closure schemes in which the diffusion coefficient profile is an empirical function of both the surface fluxes and fractional height within the boundary layer. The turbulence variables are diagnosed based on the diffusion coefficient, local gradient, and a non-local gradient correction term. The major difference between the two schemes is that the entrainment processes is explicitly considered in the YSU.

The UW01 and UW09 are the local, 1.5-order closure schemes in which the turbulent kinetic energy (TKE) is predicted or diagnosed, and other turbulence variables are diagnosed based on the local TKE. The major difference between the two schemes is the calculation method of the TKE. For more details on the four PBL schemes, please refer to the references.

In the 3D RegCM4, the surface layer scheme is imbedded in the land surface model. Because the land surface model is not activated in this study, a simple surface layer scheme is added in the SCM, which is extracted from the BATS land model [27]. With this surface layer scheme, given the prescribed heat fluxes of 300 W m^{-2} and the calculated surface temperature from the LES simulation, the surface bulk Richardson number, drag coefficient, and fractional velocity can all be derived. The surface bulk Richardson number is dependent on surface temperature, air temperture, and surface wind. For the drag coefficient and fractional velocity, a Monin-Obukhov formulation is adopted for the stability dependence by using surface bulk Richardson number and roughness. Other surface parameters are set to the same value as in the LES model runs.

A stretched vertical coordinate is used such that finer spacing is assigned to the lower levels while coarser vertical spacing is applied at higher levels. The vertical resolution set in the control SCM run is the default 18-level set of 3D RegCM4, with the model top set at 50hPa. The vertical grid size is approximately 80 m near the surface and 900 m near the 3 km height above the surface. In this set, the SCM runs are called HB, YSU, UW01, and UW09. Another vertical resolution set is the 41 level, which is used to detect how the vertical resolution affects the simulations, with a vertical grid size of approximately 80 m near the surface and 250 m near the 3 km height above the surface, and with the model top set at 50hPa. This 41-level set is the default option for the high-resolution run of 3D RegCM4. In this set, the SCM runs are called HB_z41, YSU_z41, UW01_z41, and UW09_z41, which is in contrast with the 18 level runs. All initial conditions and the model integration set in the SCM runs are the same as those in the LES.

2.4 *Diagnostic output*

2.4.1 PBL HEIGHT (ZPBL), DEPTH OF MIXED LAYER (HML), AND MIXING INDEX (MI)

Determining the PBL height (Z_{PBL}) is important in atmospheric numerical models because Z_{PBL} is used in both the PBL scheme itself (e. g., to scale the eddy diffusivity in the HB and YSU scheme) and in other physical parameterizations where required (e.g., to scale the strength of the convective velocity scale used in the wind speed component of the sea surface fluxes [28]).

All four PBL schemes and the LES model provide the PBL heights as part of their output variables, but the computation methods are not coherent among the schemes and the LES. Since the calculation method in a particular PBL scheme is a characteristic of the scheme, we first analyze the diagnosed PBL height directly from the five experiments (Z^0_{PBL}). Because Z^0_{PBL} depends on the diagnosis method used in different PBL schemes and LES [15, 29], during post processing the unified diagnosis method is added to derive the re-diagnosed PBL height (Z^1_{PBL}) of all PBL schemes and LES for comparison. The bulk Richardson number method is applied to re-diagnose the PBL height using data from all SCM and LES model simulations. In this method, the PBL height is set as the height z when bulk Richardson number between z and surface is equal to 0.25. With this method, the Z^1_{PBL} is not restricted to the model levels, indicating that it is not very sensitive to the distribution and resolution of the vertical layers, especially in lower vertical resolution cases.

Following Wang et al. [15], two extra variables are calculated, which describe the uniformity of a mixed PBL, the thickness of the well-mixed layer (H_{ML}) and mixing index (MI). A well-mixed layer is defined as the layer with a very small vertical gradient (the absolute value less than 0.20 K km^{-1}) of potential temperature. During the calculation of H_{ML}, the top and bottom of the well-mixed layer is not restricted to the vertical levels but can be intepolated between levels. The MI is measured by the standard vertical deviation of potential temperature within the well-mixed layer divided by the H_{ML}, then multipled by 10 to make the value more readable.

2.4.2 VERTICAL FLUXES AND ENTRAINMENT FLUX

The vertical fluxes of sensible heat could not be obtained from the PBL schemes in the SCM directly. For

comparison purposes, the vertical sensible heat flux $\langle w\,\theta\rangle_z$ at a certain height (z) is calculated by integrating the PBL θ tendency $\left(\frac{\partial\theta}{\partial t}\right)_{\mathrm{PBL}}$ from the surface to height z, which is as follows:

$$\langle w\,\theta\rangle_z = \langle w\,\theta\rangle_{z=0} - \int_0^z \left(\frac{\partial\theta}{\partial t}\right)_{\mathrm{PBL}} \mathrm{d}z \qquad (1)$$

where $\langle w\,\theta\rangle_{z=0}$ is the surface sensible heat flux. The entrainment flux of the sensible heat is estimated as the minimum sensible heat flux near the PBL top, and the entrainment zone is the layer with a negative sensible heat flux. As mentioned in Wang et al.[15], a disadvantage of this derivation method is the accumulation of numerical errors during the vertical integration, but these errors within the PBL are quite small in our study.

3 RESULTS

The LES simulation shows that the frictional velocity, u_*, decreases over time (Fig. 1a). All four SCM experiments in the 18-level sets can simulate the changes in u_*; however, the SCM simulated u_* is slightly smaller than the LES simulated result with biases of -0.04 m s^{-1} ~ 0.01 m s^{-1}. The simulated u_* values from the UW09 are closest to the LES results (Fig. 1a). Generally, the difference between the two vertical resolution sets is very small. Compared with the 18-level runs, the curves of u_* in the 41-level runs are smoother and the discrepancies among the HB, YSU, and UW01 are much smaller; however, the magnitudes show little change (Fig. 1b). Overall, the well-simulated u_* indicates that the module of the surface layer processes has been correctly constructed.

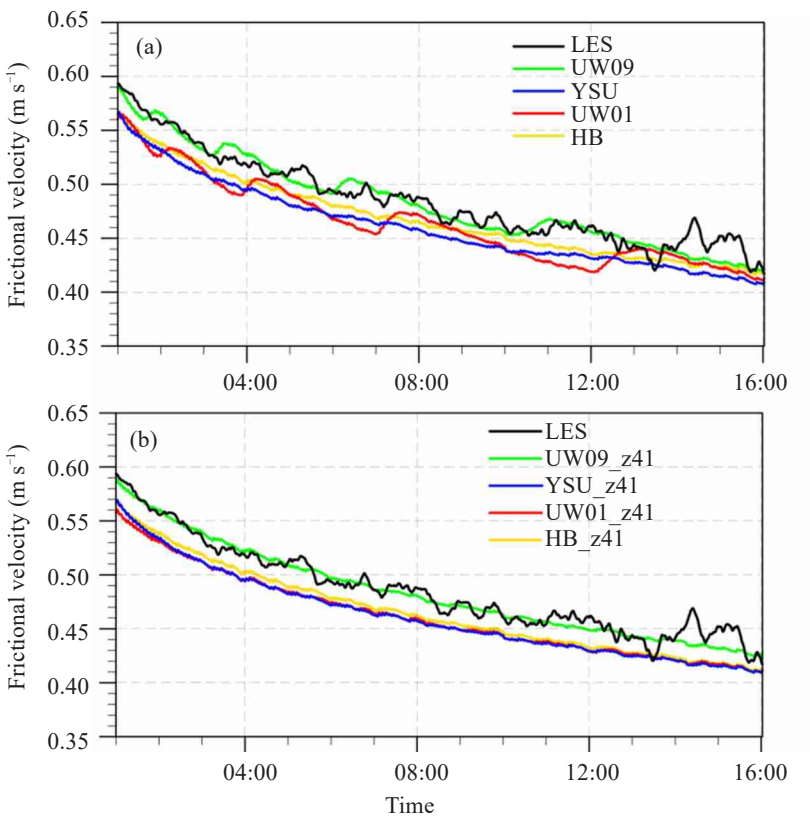

Figure 1. Time series of simulated surface frictional velocity (m s^{-1}): (a) 18-level runs and (b) 41-level runs. The simulated results are from the LES (black), HB/HB_z41 (golden), UW01/UW01_z41 (red), YSU/YSU_z41 (blue), and UW09/UW09_z41 (green) experiments.

3.1 *PBL height*

Figure 2a shows the diagnostic output, Z^0_{PBL}, which is directly from the respective PBL schemes with 18-level set and the LES run. The top of PBL is raised continuously due to the persistent surface heating during the simulation. In general, the time evolution of PBL height is well reproduced by the SCM simulations using all schemes. However, the magnitudes and smoothness of the curves are quite different among the four schemes. In the HB and YSU schemes, the PBL height for unstable conditions is determined to be the first neutral level by checking the bulk Richardson number, which is calculated between the lowest model level and the levels above. This approach permits the PBL top to lie between model levels and evolve continuously over time. In the LES run, the PBL height is defined by the height of the maximum potential temperature gradient, which has a time series that is also quite smooth due to the very high vertical resolution. However, in the UW01 and UW09 schemes, the height is restricted to lie on the model

levels, and thus, the time evolution is not continuous (can also be seen in Fig. 4 of Grenier and Bretherton [24]).

After re-diagnosed using the same methods, the Z^1_{PBL} in the SCM is more consistent with that in the LES, for both the time evolution and magnitude (Fig. 2c). All SCM results overestimate the PBL height, and the bias from the HB scheme is the largest. The higher vertical resolution does not change much, the curves of Z^0_{PBL} and Z^1_{PBL} are smoother, and the HB scheme is still the least skillful one in the 41-level runs (Figs. 2b and 2d).

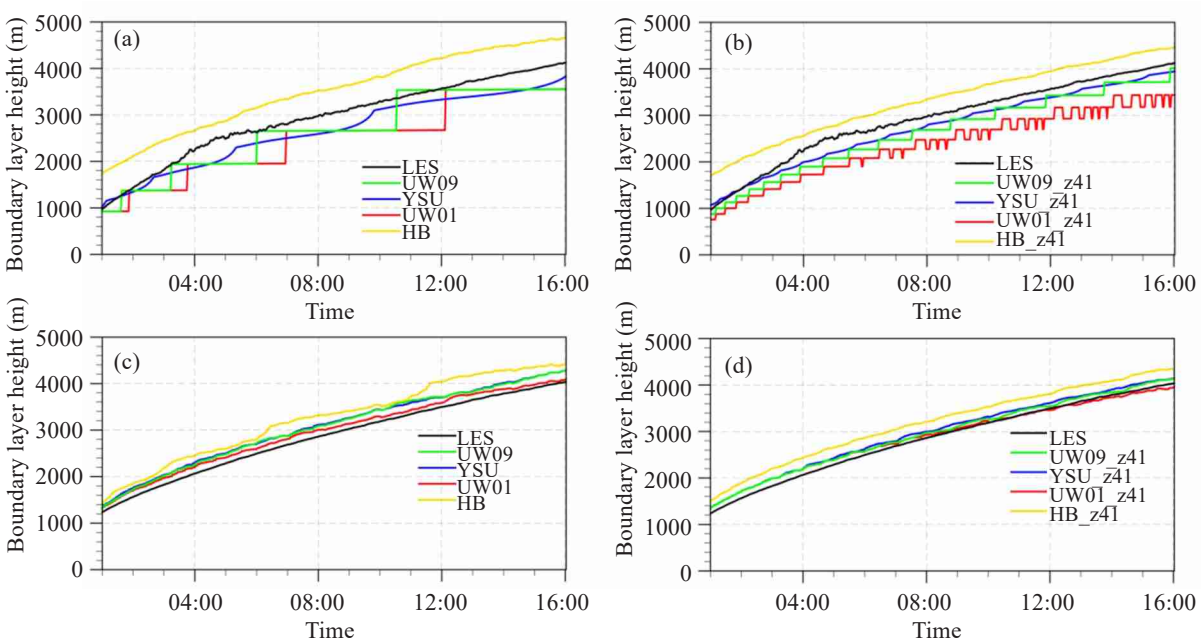

Figure 2. Time series of simulated PBL height (m): (a, c) 18-level runs and (b, d) 41-level runs. The PBL heights are diagnosed using two methods: (a, b) output directly from respective schemes and LES and (c, d) re-diagnosed using the bulk Richardson number method.

3.2 *Wind and temperature*

Figures 3a and 3b show comparisons of the vertical profiles of the hourly mean wind speeds at 5 h and 9 h from all 18-level SCM simulations. As shown by the LES simulation at 5 h in Fig. 3a, the wind speed near the surface and PBL top increases with height due to surface drag and entrainment, respectively, while the speed within the mixed layer is nearly constant due to being well mixed. At 9 h, with the PBL top rising, the mean wind speed within the well-mixed PBL decreases over time due to the synergic effect of surface drag and PBL mixing (Fig. 3b). These features are well simulated by the UW01, UW09, and YSU experiments, and the profiles are similar among all three runs. However, the simulated wind speed within the mixed layer from the HB experiment is not well mixed, and there is a large vertical gradient, because the non-local gradient correction term is not included in the momentum prognostic equation [30].

Figure 3c shows the wind profiles after raising the vertical resolution. There are larger differences among the four SCM-simulated wind profiles when compared with the lower resolution runs. Raising the vertical resolution in the lower atmosphere improves the simulation of the wind profiles for the YSU and UW09 schemes. The YSU_z41 produces the best simulation among the four schemes, while in the UW09_z41, the wind speed simulated below the boundary layer top is still slightly underestimated. For the UW01 and HB schemes, the use of a higher vertical resolution does not change much. The entrainment zone is much lower in the UW01_z41 and much higher in the HB_z41 compared with that in the LES result, and the HB is still the least skillful scheme, as the vertical gradient bias has not been reduced much.

Figures 4a and 4b show the hourly mean potential temperature profiles at 5 h and 9 h from all SCM simulations with the 18-level set. As shown by the LES simulation at 5 h in Fig. 4a, there is an unstable layer in the lower part of the PBL, a well-mixed layer with small potential temperature gradient in the mid-PBL, and a stable layer in the upper part of the PBL. At 9 h, with the PBL top rising, the mean potential temperature within the mid-PBL increases (Fig. 4b). The main discrepancies from different schemes with the 18-level set lie in the thickness of the well-mixed layer and potential temperature gradient within the well-mixed layer (Figs. 4a and 4b). Generally, the UW01, UW09, and YSU simulations are similar to each other, and the HB simulations produce the largest discrepancy relative to the LES results. In the HB, the potential temperature gradient within the mixed layer is largely overestimated, and there is a weak inversion layer between the surface layer and mixed layer, which is a fake inversion layer

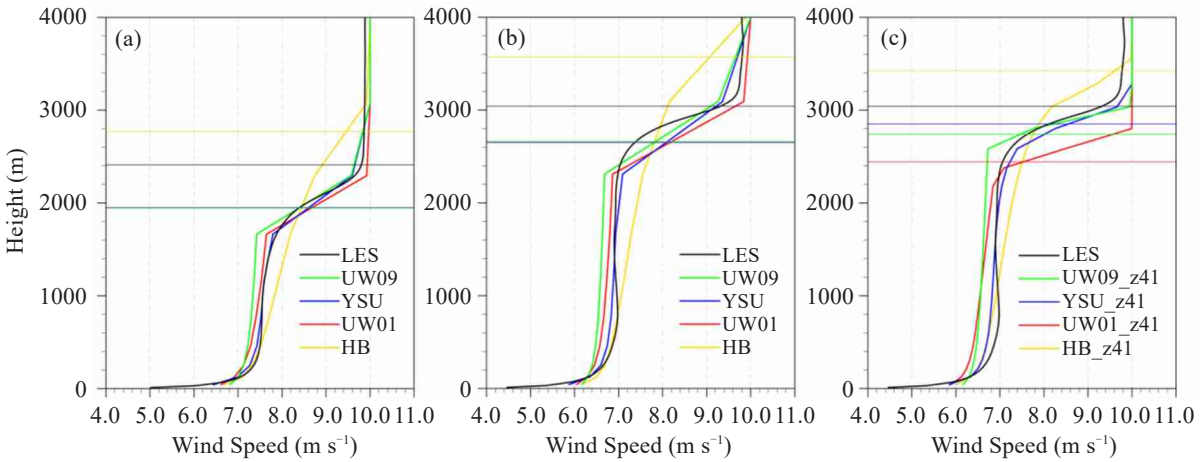

Figure 3. Simulated wind speed (units: m s^{-1}) profiles at (a) 5 h with the 18-level set, (b) 9 h with the 18-level set, and (c) 9 h with the 41-level set. In all panels, the horizontal lines denote the boundary layer top, which is output directly from respective SCM schemes and LES. In both (a) and (b), the horizontal green, blue, and red lines overlap.

and is more intense at 5 h.

Raising the vertical resolution in the lower atmosphere aids simulation of the vertical structures in the potential temperature profiles (Fig. 4c). Both the YSU and UW09 can produce nearly the same vertical profiles as that of the LES. For the UW01 and HB schemes, there are still large biases. Compared with the LES results, the PBL is more unstable and shallower in the UW01_z41 and more stable and deeper in the HB_z41. In addition, the temperature of the lower atmosphere in the UW01 scheme tends to be colder, and the temperature in the HB scheme tends to be warmer, which may correspond to the warm bias reduction in the long-term climate simulation when the PBL scheme is changed from the HB to the UW01 [30]. There is still a fake inversion layer between the surface layer and mixed layer in the HB_z41, which is more intense than that in the lower vertical resolution simulation and exists all the time (figures not shown). This fake inversion layer is due to a deficient paramerization of the eddy diffusivity in the HB scheme, which will be further discussed in the following paragraphs.

Table 2 shows a comparison of the H_{ML} and MI values from all simulations at 5 h and 9 h, which are calculated based on the hourly mean profiles. There are large biases in these two variables from the SCM results with the 18-level set, which is partly due to the low vertical resolution, because most of the biases are reduced after raising the vertical resolution. In both SCM runs with 18- and 41-level sets, the H_{ML} and MI values from the YSU are closest to those from the LES, indicating a more uniformaly mixed PBL among those SCM results. This could be attributed to both the non-local mixing and entrainment parameterization in the YSU scheme. The UW09 is also well mixed, and the bias is greatly reduced after raising the vertical resolution. The biases in the HB and UW01 schemes with the 41-level run are still large, which is consistent with the conclusion from the profile evalutions.

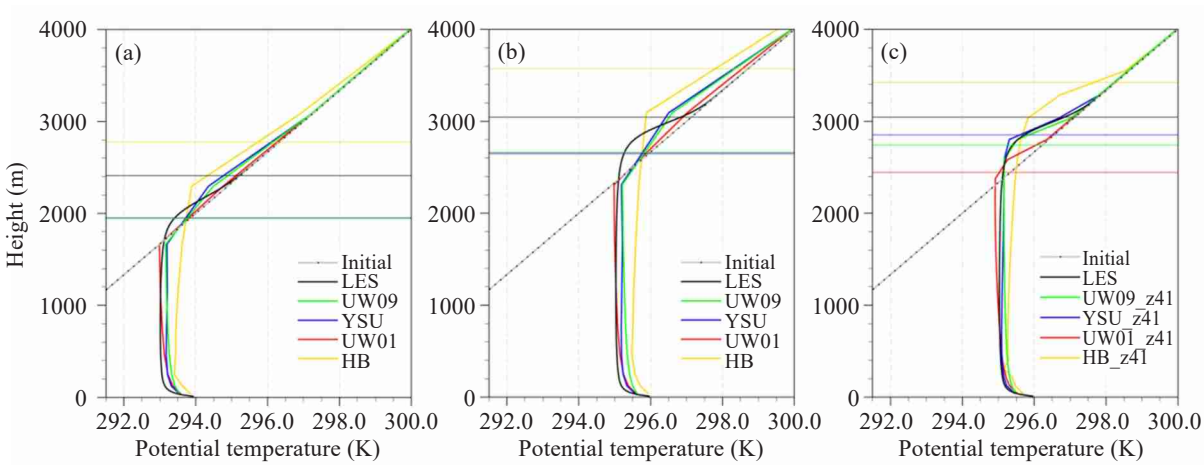

Figure 4. Simulated potential temperature (units: K) profiles at (a) 5 h with the 18-level set, (b) 9 h with the 18-level set, and (c) 9 h with the 41-level set. In all panels, the horizontal lines denote the boundary layer top, which is output directly from the respective SCM schemes and LES. In both (a) and (b), the horizontal green, blue, and red lines all overlap.

Table 2. Comparisons of the thickness of well-mixed layer (H_{ML}) and mixing index (MI) caculated based on the hourly mean profiles. The values with the two smallest biases in a column are bolded, and the value with the smallest bias is also marked with an asterisk.

Experiment	H_{ML} (m)		MI (0.1 K km^{-1})	
	5h	9h	5h	9h
LES	1218.9	1970.2	0.11	0.08
HB/HB_z41	793.5/714.0	**1586.3***/1752.1	1.27/0.86	**0.27**/0.34
YSU/YSU_z41	**965.8***/**1422.8**	**1473.2**/**2135.6**	**0.58***/**0.18***	**0.14***/**0.12***
UW01/UW01_z41	696.3/794.6	1215.7/1629.3	0.82/0.45	0.52/0.36
UW09/UW09_z41	**800.8**/**1281.1***	1343.3/**2017.5***	**0.79**/**0.28**	0.52/**0.19**

3.3 *Flux of sensible heat*

Figure 5a and 5b show hourly mean vertical fluxes of sensible heat at 5 h and 9 h with the 18-level SCM and LES, referred to as the ratio of vertical flux and surface flux. In the LES model, the ratio of PBL top entrainment flux and surface flux is approximately −0.2, which is consistent with lots of previous studies [15−18, 22], indicating the entrainment flux is about −60 W m^{-2} (−0.2 × 300 W m^{-2}). It shows that the UW01, UW09, and YSU produce less downward entrainment buoyancy flux at the PBL top, while the HB scheme produces more flux. Among the schemes, the value from the YSU scheme is closest to the LES value. All schemes overestimate the height of the minimum buoyancy flux. Partly due to the numerical error from the integral calculation of the vertical flux in the SCM, the flux value cannot be quickly reduced to around zero above the top of PBL. These features can also be clearly seen from the time evolution figure (Figs. 6a, 6c, 6e, and 6g). The Z^0_{PBL} is close to the height of the minimum buoyancy flux, especially in the UW01 and UW09 schemes, and it helps to indicate the time evolution of the entrainment zone height. Overestimations of the entrainment flux at the PBL top always exist in the HB scheme (Fig. 6a).

After the vertical resolution being raised, the entrainment zones are better resolved in all schemes (Fig. 5c). The YSU remains the scheme with the lowest bias of heat flux, while the HB_z41 overestimates the entrainment flux and height of the entrainment zone, and the UW01_z41 and UW09_z41 underestimate both. As shown in the time evolution figure, the biases of the heat flux change little over time (Figs. 6b, 6d, 6f, and 6h).

3.4 *Eddy diffusivity and TKE*

Figure 7a shows the eddy diffusivity profiles for heat (K_h) after 5 h with the 18-level set. All results have a 5-min average. This result shows that the difference in the K_h magnitude among the schemes is very large. The largest diffusivities appear in the UW09 scheme with a vertical maximum $K_h \approx 1500$ m^2, and the maximum K_h values vary from 500 to 900 m^2 s^{-1} in other schemes. The K_h profiles shown here only characterize the local mixing ability in the HB and YSU schemes because other part of the turbulent mixing in these schemes is also represented by their non-local mixing treatments. Therefore, the shapes of K_h in the HB and YSU are quite different from those in the UW01 and UW09 schemes, and the location of the maximum diffusivity values are lower. The differences in the shape are more obvious in

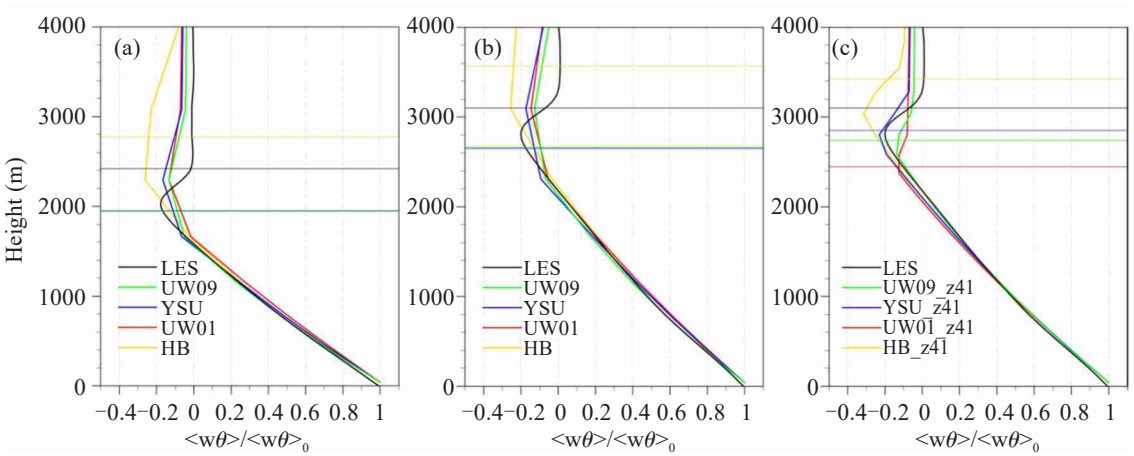

Figure 5. Simulated vertical sensible heat flux (normalized by the surface flux) profiles at (a) 5 h with the 18-level set, (b) 9 h with the 18-level set, and (c) 9 h with the 41-level set. In all panels, the horizontal lines denote the boundary layer top, which is output directly from the respective SCM schemes and LES. In both (a) and (b), the horizontal green, blue, and red lines all overlap.

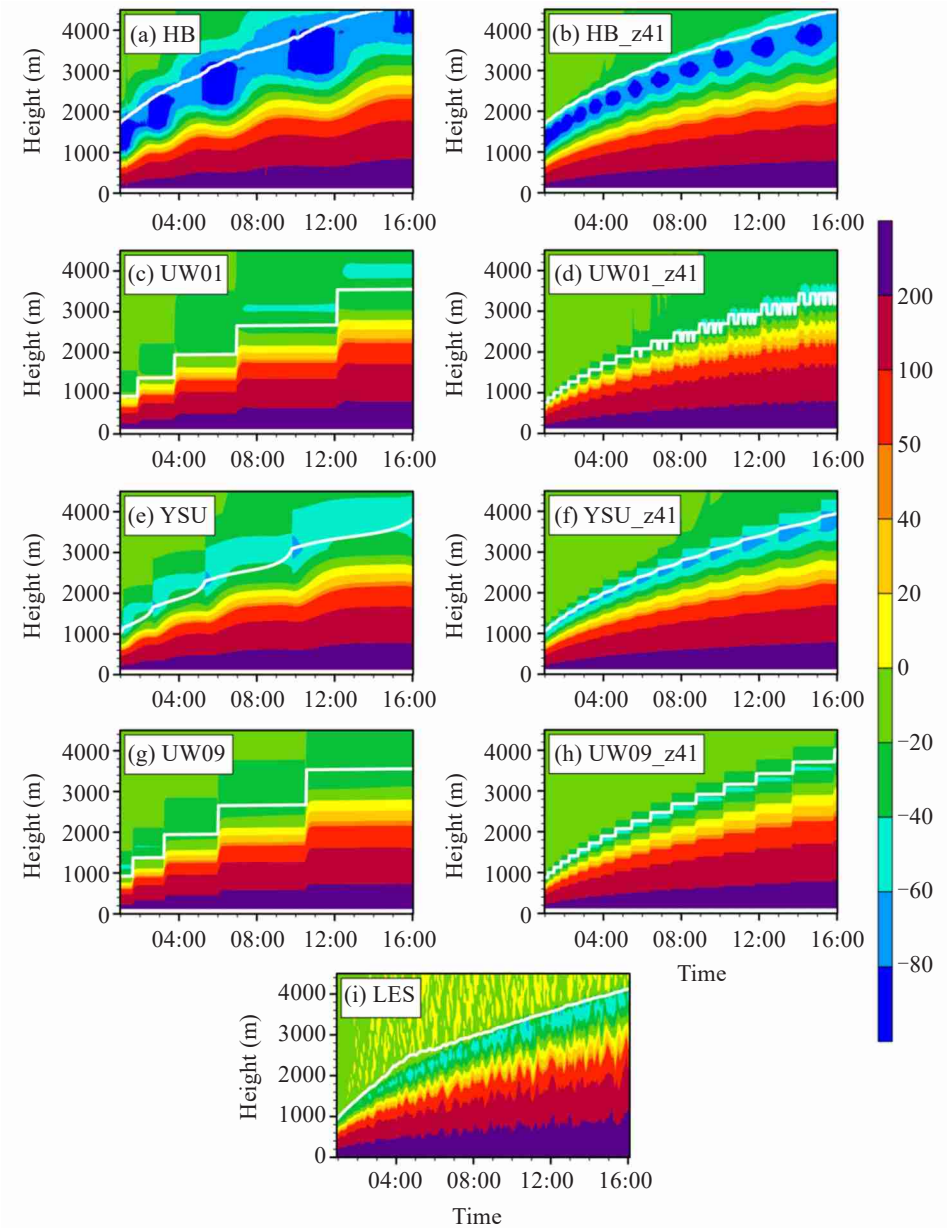

Figure 6. Time evolution of the vertical profiles of sensible heat fluxes (units: W m^{-2}) from (a) HB, (b) HB_z41, (c) UW01, (d) UW01_z41, (e) YSU, (f) YSU_z41, (g) UW09, (h) UW09_z41, and (i) LES. White lines denote the boundary layer top, which is output directly from the respective SCM schemes and LES run.

the 41-level set (Fig. 7b).

The time evolution figures (Figs. 8a, 8c, 8e, and 8g) show that as the PBL top raises, the maximum values of K_h generally increase over time, and diffusivities larger than 10 m^2 s^{-1} also extend to higher levels. Diffusivity profiles are limited below Z_{PBL} in all schemes because the K_h profiles are parameterized as so, although the detailed formulations of K_h are different among the four schemes. Compared with the smooth evolutionary features at high resolution (Figs. 8b, 8d, 8f, and 8h), the low resolution results show a fluctuating evolution, synchronizing with the change in Z_{PBL}.

Figures 7c and 7d present the vertical distribution of the Prandtl number, where $Pr = K_m/K_h$. In the surface layer and mixed layer, the Pr values from all schemes except the YSU are nearly constant and smaller than 1.0, while the Pr value in the YSU increases upward. Above the mixed layer, in both the HB and UW09 schemes, the Pr decreases to 1.0; and in the UW01 scheme, the Pr decreases to a constant value larger than 1.0; while in the YSU scheme, the Pr profile is quite different, showing that within the entrainment zone the Pr increases beyond 1.0, but above the PBL top the Pr decreases to 1.0 quickly.

Near the surface layer top, there is significant discontinuity on the Pr in the HB scheme due to different Pr equations being used between the surface layer and mixed layer as follows:

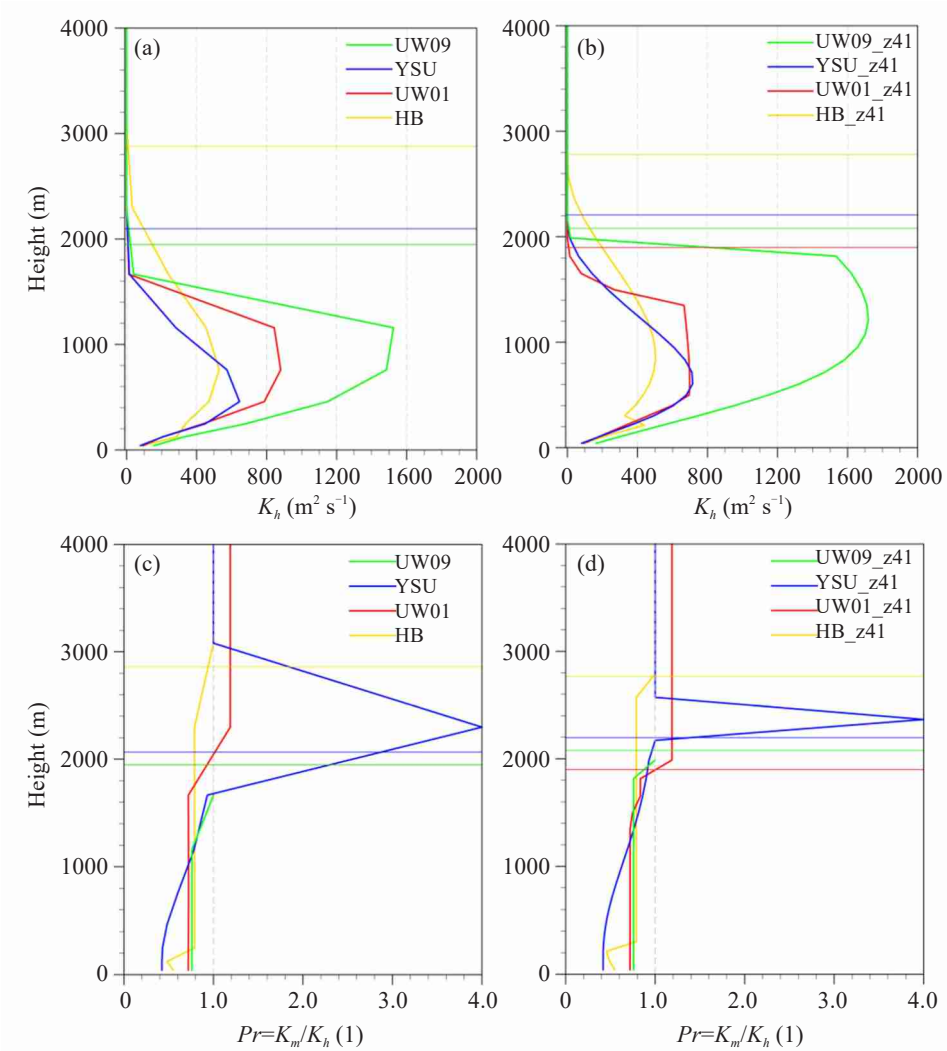

Figure 7. Simulated (a, b) eddy diffusivity profiles for heat (units: m^2 s^{-1}) and (c, d) the Prandtl number at 5 h with (a, c) the 18-level set and (b, d) the 41-level set. In all panels, the horizontal lines denote the boundary layer top, which is output directly from the respective SCM schemes. In both (a) and (c), the horizontal green and red lines overlap.

$$Pr = Pr_{\mathrm{ML}} = \frac{\phi_h}{\phi_m}\left(\frac{0.1{*}Z_{\mathrm{PBL}}}{L}\right) + a{*}k{*}\frac{0.1{*}Z_{\mathrm{PBL}}}{Z_{\mathrm{PBL}}} = \left(1 - 15{*}\frac{0.1{*}Z_{\mathrm{PBL}}}{L}\right)^{-\frac{1}{6}} + 0.34,$$

$$\text{when } z \geqslant 0.1{*}Z_{\mathrm{PBL}}$$

$$Pr = \frac{\phi_h}{\phi_m}\left(\frac{z}{L}\right) = \left(1 - 15{*}\frac{z}{L}\right)^{-\frac{1}{6}},$$

$$\text{when } z < 0.1{*}Z_{\mathrm{PBL}} \qquad (2)$$

where z is the height, L is the Monin-Obukhov length scale, $\phi_h(z) = \left(1 - 15{*}\frac{z}{L}\right)^{-\frac{1}{2}}$, $\phi_m(z) = \left(1 - 15{*}\frac{z}{L}\right)^{-\frac{1}{3}}$, a = 0.85, and k is the von Karman constant (= 0.4). Therefore, there is a discontinuity at the top of the surface layer (z = 0.1*Z_{PBL}), where the Pr drops from a constant value Pr_{ML} in the mixed layer to Pr_{ML} − 0.34 at the top of the surface layer and then increases towards the surface. At the same height, the discontinuity occurs in the K_h profile, which is more obvious in the higher vertical resolution set (Figs. 7b and 8b). This induces the fake inversion in the potential temperature profile, which was mentioned in the previous paragraphs (Fig. 4c). Till now, the vertical variation of Pr throughout the PBL is still less known, and usually a presumed profile shape is given and adjusted by matching the simulated heat flux profiles from the SCM results with the LES data [31]. Therefore, the significant discontinuity on the Pr in the HB scheme is suggested to be removed in order to reduce the biases in heat flux and potential temperature.

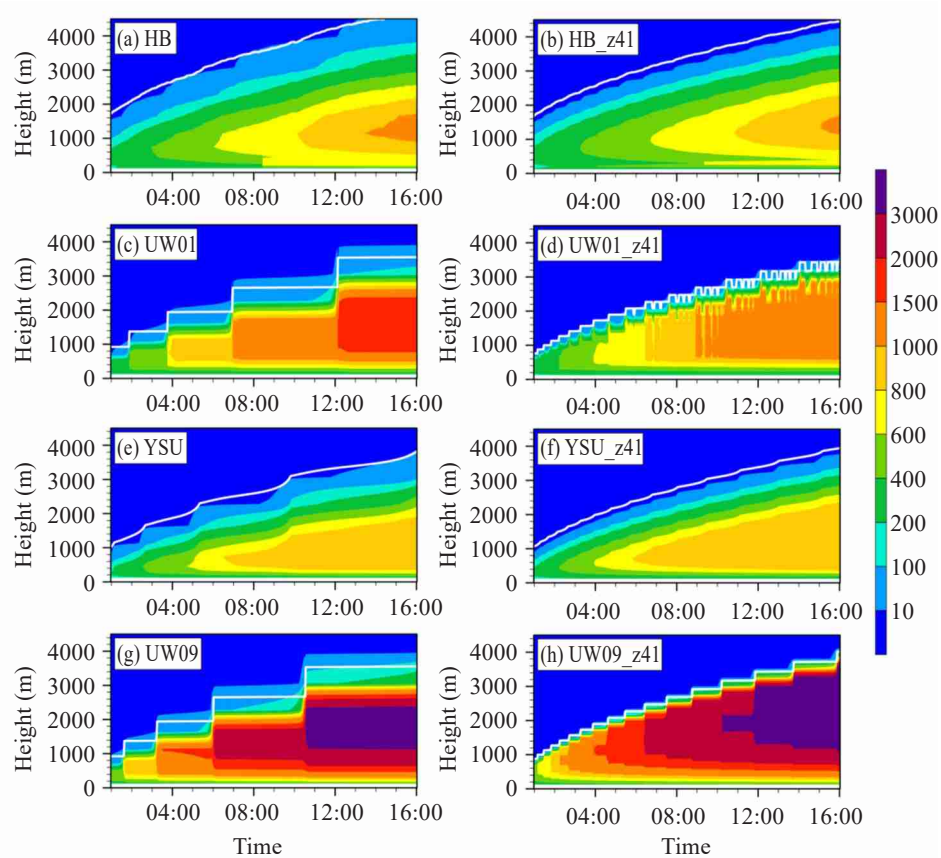

Figure 8. Time evolution of the vertical profiles of eddy diffusivity for heat (units: $m^2\ s^{-1}$) from (a) HB, (b) HB_z41, (c) UW01, (d) UW01_z41, (e) YSU, (f) YSU_z41, (g) UW09, and (h) UW09_z41. White lines denote the boundary layer top, which is output directly from respective SCM schemes.

Figures 9a and 9b show TKE vertical profiles from the 18-level SCM simulations using UW01 and UW09 schemes and LES simulation. The LES model results show that the high TKE values appear in both the surface layer and mid-PBL, and the TKE value rapidly decreases due to the stable stratification near the PBL top. In the UW01 and UW09 schemes, the high TKE values in the suface layer cannot be captured. Above the surface layer, the TKE profiles in two schemes have a similar shape to that of the LES; however, the magnitudes are underestimated with biases of approximately 30%. In these two schemes, the minimum TKE above the PBL is zero, which is approximately 0.3 $m^2\ s^{-2}$ in the LES. After raising the vertical resolution, the TKE bias in the UW09 scheme is greatly reduced, while that in the UW01 scheme shows little change (Fig. 9c). These features can also be clearly seen from the time evolution figure (Fig. 10). Similar to K_h, as the PBL top raises, the maximum values of TKE generally increase, and the values greater than a certain small TKE (e.g., 0.5 $m^2\ s^{-2}$) extend to higher levels. The TKE biases change little over time and remain 1~1.5 $m^2\ s^{-2}$ in the mixed layer.

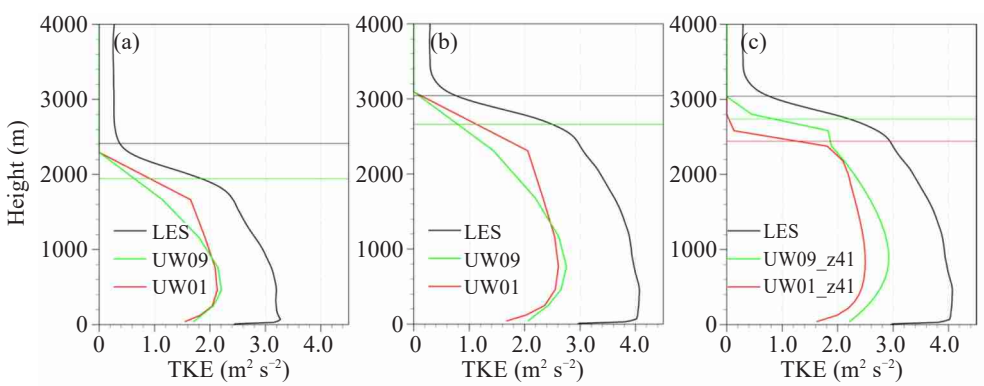

Figure 9. Simulated TKE (units: $m^2\ s^{-2}$) at (a) 5 h with the 18-level set, (b) 9 h with the 18-level set, and (c) 9 h with the 41-level set. Horizontal lines denote the boundary layer top, which is output directly from respective SCM schemes and LES. In both (a) and (b), the horizontal green and red lines overlap.

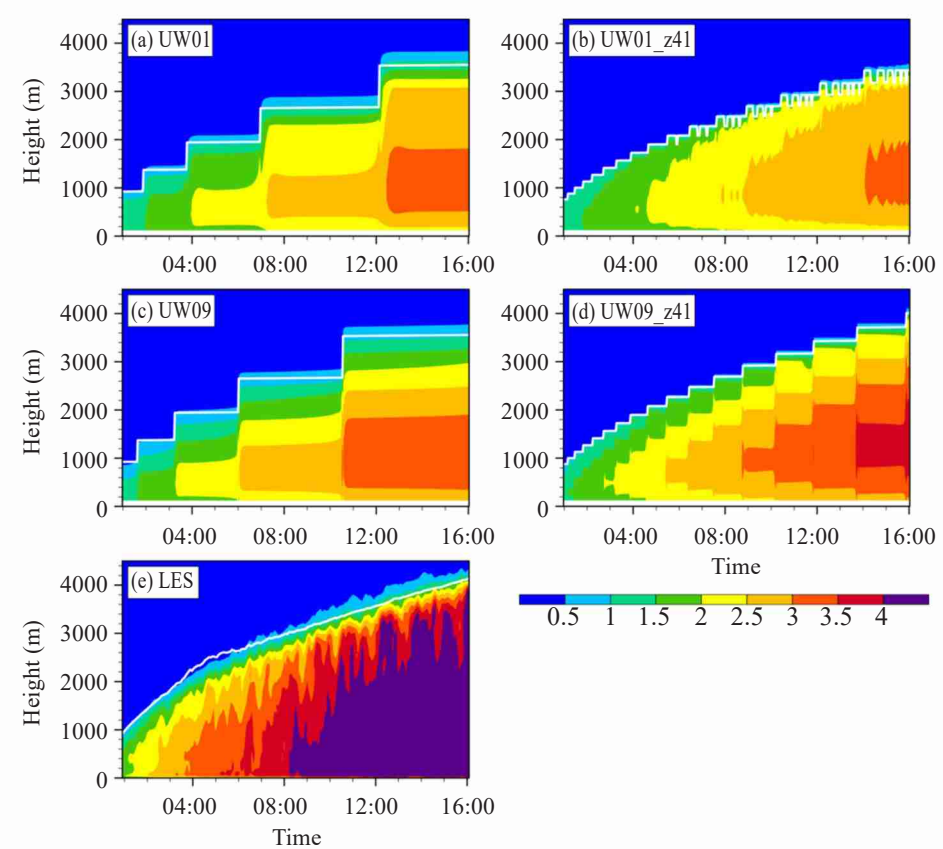

Figure 10. Time evolution of the vertical profiles of TKE (units: $m^2\ s^{-2}$) from (a) UW01, (b) UW01_z41, (c) UW09, (d) UW09_z41, and (e) LES. White lines denote the boundary layer top, which is output directly from respective SCM schemes.

4 SUMMARY

An SCM based on parameterizations and the dynamic core inherited from the RegCM4 was successfully constructed. With the LES benchmark simulation results, the SCM model was tested in DCBL simulations. Despite the successful general DCBL simulations, discrepancies within individual SCM simulations do exist. Specifically, four PBL schemes (two of which were added into the SCM in this study) were further compared in terms of their performances for the PBL height, mixing strength, and vertical profiles of potential temperature, wind speed, sensible heat flux, eddy diffusivity, and TKE. The vertical resolution effect on the simulations was also discussed.

The diagnosed PBL height directly from the SCM is quite different among the four schemes due to the use of different calculation methods, which should not be used alone as an evaluation indicator. However, the PBL height can aid indicating the time evolution of the entrainment zone height and vertical profiles of the heat flux, eddy diffusivity, and TKE. For the re-diagnosed PBL height using the same method, there is little difference among the schemes except for the HB, and the biases relative to the LES result are small, indicating a successful general simulation with the DCBL.

In general, the YSU performs best in reproducing the LES results on nearly all variables evaluated, but the YSU still has considerable potential for improvement. The major bias is that the wind speed simulated in the YSU is not as well mixed as that in the LES, which is also a common problem in all four schemes. The UW09 scheme has the second best performance. The wind speed simulated in the UW09 below the boundary layer top is slightly underestimated. The UW09 also underesimates the TKE, entrainment flux, and height of the entrainment zone. The UW01 ranks third, as the biases are similar to those of the UW09 but those of the UW01 are larger, and the simulated potential temperature is underestimated and not well mixed in the UW01.

The HB is the least skillful scheme. The major biases include the following: (1) The PBL height, entrainment flux, and height of the entrainment zone are overestimated. (2) The vertical gradients of the potential temperature and wind speed within the mixed layer are largely overestimated. (3) Due to a deficient paramerization of *Pr*, there is a fake inversion layer near the top of the surface layer.

Raising the vertical resolution in the lower atmosphere aids the simulation of the potential temperature and sensible heat flux profiles for all the schemes. However, if the simulation of wind profiles is considered, a higher vertical resolution is beneficial only

for the YSU and UW09 schemes. In the 1.5-order closure schemes, UW01 and UW09, the TKE are calculated. In both two schemes, the TKE values within the PBL are underestimated in comparison with the LES model. Raising the vertical resolution helps to reduce the bias only in the UW09 scheme.

Notably, the assessments in this study focus only on a single DCBL case. The comprehensive performance assessment of a PBL scheme needs more cases, such as the cases of a stably stratified boundary layer, nocturnal stratocumulus-topped boundary layer, and real cases, which should be further studied in future work. Studies on the interaction between the PBL and moist convections, radiation processes, or surface processes are also desirable. Although further testing is needed, current simulations show encouraging results towards the use of SCM for the evaluation of simulated physical processes by the RegCM4.

REFERENCES

[1] WANG X. Development of a toy column model and its application in testing cumulus convection parameterizations [J]. Science Bulletin, 2015, 60(15): 1359-1365, https://doi.org/10.1007/s11434-015-0850-8.

[2] GIORGI F, COPPOLA E, SOLMON F, et al. RegCM4: model description and preliminary tests over multiple CORDEX domains [J]. Climate Research, 2012, 52: 7-29, https://doi.org/10.3354/cr01018.

[3] HAN Z, ZHOU B, XU Y, et al. Projected changes in haze pollution potential in China: an ensemble of regional climate model simulations [J]. Atmos Chem Phys, 2017, 17 (16): 10109-10123, https://doi.org/10.5194/acp-17-10109-2017.

[4] DU Yao-dong, YANG Hong-long, CAO Chao-xiong, et al. Future change of precipitation extremes over the Pearl River Basin from regional climate models [J]. J Trop Meteor, 2016, 24(1): 57-65, https://doi. org / 10.16555 / j.1006-8775.2016.01.007.

[5] GAO X, GIORGI F. Use of the RegCM system over East Asia: Review and perspectives [J]. Engineering, 2017, 3 (5): 766-772, https://doi.org/10.1016/J.ENG.2017.05.019.

[6] ZOU L, ZHOU T, LIU H. Performance of a high resolution regional ocean-atmosphere coupled model over western North Pacific region: sensitivity to cumulus parameterizations [J]. Clim Dyn, 2019, 53(7): 4611-4627, https://doi.org/10.1007/s00382-019-04812-2.

[7] WU Jie, GAO Xue-jie. Simulation of tropical cyclones over the Western North Pacific and landfalling in China by RegCM4 [J]. J Trop Meteor, 2019, 25(4): 437-447, https:// doi/org/ 10.16555/j.1006-8775.2019.04.002.

[8] MORRISON H, SHUPE M D, CURRY J A. Modeling clouds observed at SHEBA using a bulk microphysics parameterization implemented into a single-column model [J]. Journal of Geophysical Research: Atmospheres, 2003, 108(D8): 4255, https://doi.org/10.1029/2002JD002229.

[9] YANG J, SHEN X. The construction of SCM in GRAPES and its applications in two field experiment simulations [J]. Adv Atmos Sci, 2011, 28(3): 534-550, https://doi. org / 10.1007/s00376-010-0062-8.

[10] HONG S-Y, PARK H, CHEONG H-B, et al. The Global/ Regional Integrated Model system (GRIMs) [J]. Asia-Pacific J Atmos Sci, 2013, 49(2): 219-243, https://doi.org/ 10.1007/s13143-013-0023-0.

[11] NEGGERS R A J, SIEBESMA A P, HEUS T. Continuous single-column model evaluation at a permanent meteorological supersite [J]. Bull Amer Meteorol Soc, 2012, 93(9): 1389-1400, https://doi. org / 10.1175 / BAMS-D-11-00162.1.

[12] DENG A, SEAMAN N L, KAIN J S. A shallow-convection parameterization for mesoscale models, Part I: Submodel description and preliminary applications [J]. Journal of the Atmospheric Sciences, 2003, 60(1): 34-56, https://doi. org / 10.1175 / 1520-0469(2003)060<0034: ASCPFM>2.0.CO;2.

[13] HACKER J P, SNYDER C. Ensemble Kalman filter assimilation of fixed screen-height observations in a parameterized PBL [J]. Mon Wea Rev, 2005, 133(11): 3260-3275, https://doi.org/10.1175/MWR3022.1.

[14] COHEN A E, CAVALLO S M, CONIGLIO M C, et al. A review of planetary boundary layer parameterization schemes and their sensitivity in simulating southeastern US cold season severe weather environments [J]. Wea Forecasting, 2015, 30(3): 591-612, https://doi. org / 10.1175/WAF-D-14-00105.1.

[15] WANG W, SHEN X, HUANG W. A comparison of boundary-layer characteristics simulated using different parametrization schemes [J]. Boundary Layer Meteorol, 2016, 161(2): 375-403, https://doi. org / 10.1007 / s10546-016-0175-4.

[16] BRETHERTON C S, PARK S. A new moist turbulence parameterization in the Community Atmosphere Model [J]. J Climate, 2009, 22(12): 3422-3448, https://doi. org / 10.1175/2008JCLI2556.1.

[17] NOH Y, CHEON W G, HONG S Y, et al. Improvement of the K-profile model for the planetary boundary layer based on large eddy simulation data [J]. Boundary Layer Meteorol, 2003, 107(2): 401-427, https://doi.org/10.1023/ A:1022146015946.

[18] SHIN H H, DUDHIA J. Evaluation of PBL parameterizations in WRF at subkilometer grid spacings: turbulence statistics in the dry convective boundary layer [J]. Mon Wea Rev, 2016, 144(3): 1161-1177, https://doi. org/10.1175/MWR-D-15-0208.1.

[19] STEVENS B, MOENG C-H, ACKERMAN A S, et al. Evaluation of large-eddy simulations via observations of nocturnal marine stratocumulus [J]. Mon Wea Rev, 2005, 133(6): 1443-1462, https://doi.org/10.1175/MWR2930.1.

[20] HOLTSLAG A A M, DE BRUIJN E I F, PAN H L. A high resolution air mass transformation model for short-range weather forecasting [J]. Mon Wea Rev, 1990, 118(8): 1561-1575, https://doi.org/10.1175/1520-0493(1990)118< 1561:AHRAMT>2.0.CO;2.

[21] HOLTSLAG A A M, BOVILLE B A. Local versus nonlocal boundary-layer diffusion in a global climate model [J]. J Climate, 1993, 6(10): 1825-1842, https://doi. org / 10.1175 / 1520-0442(1993)006<1825: LVNBLD>2.0. CO;2.

[22] HONG S-Y, NOH Y, DUDHIA J. A new vertical diffusion package with an explicit treatment of entrainment processes [J]. Mon Wea Rev, 2006, 134(9): 2318-2341, https://doi.org/10.1175/MWR3199.1.

[23] HONG S Y. A new stable boundary-layer mixing scheme

and its impact on the simulated East Asian summer monsoon [J]. Quart J Roy Meteorol Soc, 2010, 136(651): 1481-1496, https://doi.org/10.1002/qj.665.

[24] GRENIER H, BRETHERTON C S. A moist PBL parameterization for large-scale models and its application to subtropical cloud-topped marine boundary layers [J]. Mon Wea Rev, 2001, 129(3): 357-377, https://doi. org / 10.1175 / 1520-0493(2001)129<0357: AMPPFL>2.0.CO;2.

[25] BRETHERTON C S, MCCAA J R, GRENIER H. A new parameterization for shallow cumulus convection and its application to marine subtropical cloud-topped boundary layers, Part I: Description and 1D results [J]. Mon Wea Rev, 2004, 132(4): 864-882, https://doi.org/10.1175/1520-0493(2004)132<0864:ANPFSC>2.0.CO;2.

[26] O'BRIEN T A, CHUANG P Y, SLOAN L C, et al. Coupling a new turbulence parametrization to RegCM adds realistic stratocumulus clouds [J]. Geosci Model Dev, 2012, 5(4): 989-1008, https://doi.org/10.5194/gmd-5-989-2012.

[27] DICKINSON R E, HENDERSON-SELLERS A, KENNEDY P. Biosphere-Atmosphere Transfer Scheme (BATS) version 1e as coupled to the NCAR Community Climate Model [R]. 1993, NCAR Tech Note NCAR/TN-387+STR, 72 pp, https://doi.org/10.5065/D67W6959.

[28] ZENG X, ZHAO M, DICKINSON R E. Intercomparison of bulk aerodynamic algorithms for the computation of sea surface fluxes using TOGA COARE and TAO data [J]. J Climate, 1998, 11(10): 2628-2644, https://doi. org / 10.1175/1520-0442(1998)011<2628:IOBAAF>2.0.CO;2.

[29] LEMONE M A, TEWARI M, CHEN F, et al. Objectively determined fair-weather CBL depths in the ARW-WRF model and their comparison to CASES-97 observations [J]. Mon Wea Rev, 2013, 141(1): 30-54, https://doi. org / 10.1175/MWR-D-12-00106.1.

[30] GUTTLER I, BRANKOVIĆ Č, O'BRIEN T A, et al. Sensitivity of the regional climate model RegCM4. 2 to planetary boundary layer parameterization [J]. Clim Dyn, 2014, 43(7-8): 1753-1772, https://doi.org/10.1007/s00382-013-2003-6.

[31] LI D. Turbulent Prandtl number in the atmospheric boundary layer-where are we now? [J]. Atmos Res, 2019, 216: 86-105, https://doi. org / 10.1016 / j. atmosres.2018.09.015.

Citation: HAN Zhen-yu and WANG Yu-xing. Development of a single-column model in RegCM4 and its preliminary application for evaluating PBL schemes in simulating the dry convection boundary layer [J]. J Trop Meteor, 2021, 27(3): 259-271, https://doi.org/10.46267/j.1006-8775.2021.023.